

Laser line shape and spectral density of frequency noise

G. M. Stéphan,¹ T. T. Tam,² S. Blin,¹ P. Besnard,¹ and M. Têtu³

¹*Laboratoire d'Optronique associé au Centre National de la Recherche Scientifique, ENSSAT,
6 rue Kerampont, 22305 Lannion Cedex, France*

²*College of Applied Science and Technology, Vietnam National University, Hanoi (VNUH), 144 Xuan Thuy str., Building E3, Cauaiay,
Hanoi, Vietnam*

³*DiCOS Technologies, Boul. du Parc Technologique, Bureau 200, Québec, Canada G1K 7P4*

(Received 30 June 2004; published 11 April 2005)

Published experimental results show that single-mode laser light is characterized in the microwave range by a frequency noise which essentially includes a white part and a $1/f$ (flicker) part. We theoretically show that the spectral density (the line shape) which is compatible with these results is a Voigt profile whose Lorentzian part or homogeneous component is linked to the white noise and the Gaussian part to the $1/f$ noise. We measure semiconductor laser line profiles and verify that they can be fit with Voigt functions. It is also verified that the width of the Lorentzian part varies like $1/P$ where P is the laser power while the width of the Gaussian part is more of a constant. Finally, we theoretically show from first principles that laser line shapes are also described by Voigt functions where the Lorentzian part is the laser Airy function and the Gaussian part originates from population noise.

DOI: 10.1103/PhysRevA.71.043809

PACS number(s): 42.55.Ah, 42.55.Px

I. INTRODUCTION

Direct measurements of the power spectral density of frequency noise essentially characterize lasers having high spectral purities used in metrology or in optical telecommunication. They show that the main contributions in single-mode semiconductor lasers arise from white noise and $1/f$ noise (flicker noise) [1–3]. A flicker noise has also been measured [4,5] in the intensity fluctuations of a semiconductor laser and has been the subject of many studies [6–9]. A correlation was experimentally shown [10] to exist between this noise and frequency fluctuations in the optical emission. This correlation was theoretically understood [11–13] always in a semiconductor laser from the coupling between the index of refraction n and the fluctuations of the charge carriers N due to spontaneous emission.

Beside this $1/f$ noise due to charge carriers, the frequency white noise due to spontaneous emission is well known to be the primary origin of the laser linewidth [14]: It has been theoretically modeled in the Langevin equations of the laser as a time δ -correlated term, analogous to the random Brownian collision term in the motion equations of a particle in a gas. A comprehensive review of the understanding of laser spectra is given in Ref. [15].

However, while the laser linewidth has been the subject of many studies, the laser line shape was generally assumed to be described by a Lorentzian profile. The aim of our work is essentially to demonstrate that a Voigt profile is better adapted.

For this purpose, the relation between frequency noise and laser spectrum is described in Sec. II. We show and verify that the line shape, or the spectral distribution, of a single-mode laser which is compatible with both the white and flicker noises can essentially be described by a Voigt function. Many authors have already intuitively guessed that the laser line shape can be fit by a Voigt profile [16,17] and even described it by a convolution between a Lorentzian and a Gaussian [18], which is a Voigt function. However, no

definite proof has been given up to now. In the following we first link the spectral density of the laser light to the noise spectrum: The white noise gives birth to the Lorentzian part and the $1/f$ noise is responsible for the Gaussian part. Then we verify that the Voigt function gives a nice fit to experimentally measured line shapes for a diode laser. The fit parameters are Γ , the half width at half maximum (HWHM) of the Lorentzian, and σ^2 , the variance of the Gaussian. Our experimental results show that Γ follows a $1/P$ law, where P is the laser power, while σ^2 has a slower variation. We find the relation between the optical parameters Γ and σ^2 and the noise coefficients h_0 and h_{-1} . It follows that a measurement of h_0 and h_{-1} will allow one to characterize a laser line, which is otherwise difficult to measure directly from interference effects, especially for a laser used in metrology.

In Sec. III, we make the connection between the homogeneous laser line, which is described by the Airy function of the laser [19–21], and its inhomogeneous properties, which are included in the Gaussian distribution of the resonance frequency. Among its properties, this Airy function allows one to describe both the Fabry-Perot interferometer or the laser in a continuous way, when the gain is increased across the oscillation threshold.

During the course of this calculation, Lamb's solution for the laser intensity, Henry's factor, the role of the spontaneous emission, and "technical" or electronic noises naturally appear. It is thus believed that this synthesis gives a clear understanding of the single-mode laser line shape.

II. BROADBAND FREQUENCY NOISE AND LASER SPECTRAL DENSITY

A. Noise coefficients and laser Voigt spectrum

In this paper, we do not give any experimental result on the laser frequency noise (see Ref. [3]) but we want to make a clear connection between it and the optical spectrum. This is why we schematically describe both experiments in Fig. 1

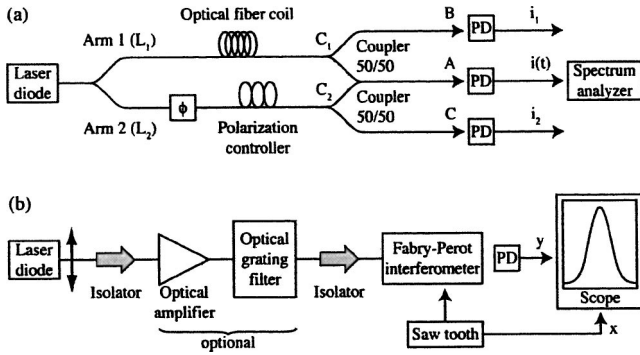


FIG. 1. (a) A practical Mach-Zehnder interferometer for the measurement of field noise properties. The fourth arms of the optical couplers are not shown. ϕ is the dephasor. (b) Optical spectrum analyzer based on a Fabry-Perot interferometer.

on noise and optical spectra and give some details on the measured quantities below.

The power density of frequency noise of a single-mode laser is measured in the standard experiment described in Fig. 1(a): A Mach-Zehnder interferometer splits the field into two parts which are directed into two different arms. A time delay τ_d is introduced with an optical fiber coil in one arm. The recombined field at the output is a function of time t and τ_d . For a fixed value of τ_d , the interferometer is used as a phase-amplitude convertor and the fringe system fluctuates in position and amplitude with time. The amplitude-converted phase noise is larger than the laser intensity noise which can be neglected in this kind of experiment. The larger τ_d is, the larger is the phase fluctuation. τ_d has to be optimized to have a comfortable signal, however in the limits of a linear approximation for a sine function (the fringe function around a zero). The optical signal is detected by a fast detector which delivers a current $i(t, \tau_d)$ which is proportional to the intensity of the field.

The output current of the detector (A) in Fig. 1(a) is written as

$$i(t, \tau_d) = i_1 + i_2 + 2\sqrt{i_1 i_2} \cos[\omega_0 \tau_d + \phi(t + \tau_d) - \phi(t)], \quad (1)$$

where i_1 and i_2 are the currents detected by the photodiodes (B) and (C) in arms 1 and 2 as shown in Fig. 1(a). i_1 and i_2 can also be detected directly by the detector (A) simply by successively cutting out arms 1 and 2 of the interferometer. The time average of $i(t, \tau_d)$ corresponds to the interferogram. The amplitude noises in i_1 and i_2 are supposed to be negligible.¹ ω_0 is the central angular frequency of the field and $\phi(t)$ is the random phase.² The signal $i(t, \tau_d)$ where τ_d is kept fixed is sent into a spectrum analyzer which delivers as

¹It follows that we are not considering any effect of the population relaxation resonance for example. Such effects are not preponderant and can be added easily in a more complete theory.

²The mean value $\bar{i}(\tau_d) = \langle i(t, \tau_d) \rangle$ with respect to time allows one to find the optical spectrum through the Wiener-Kintchin theorem. The measurement of $\bar{i}(\tau_d)$ is an easy task when the coherence length is not too large. This is not the case of metrological lasers.

its output the spectral power of current noise $\tilde{S}_i(f)$. This quantity is linked to the spectral power of the frequency noise of the field $S_{\delta\nu}(f)$ through the relation [3]

$$\tilde{S}_i(f) = (i_1 + i_2)^2 \delta(f) + 16i_1 i_2 S_{\delta\nu}(f) \frac{\sin^2(\pi f \tau_d)}{f^2}. \quad (2)$$

Here f is the Fourier frequency whose range generally extends from 10 kHz to 20 GHz. When $f \ll 1/\tau_d$, one notes that the second term has the asymptotic value $16i_1 i_2 (\pi \tau_d)^2 S_{\delta\nu}(f)$. The coefficient $16i_1 i_2 (\pi \tau_d)^2$ is a scale factor; it has to be experimentally measured. We give some definitions and steps of the calculation in Appendix A.

The optical spectrum of the field is denoted by $I_E(\omega) = \tilde{E}(\omega) \tilde{E}^*(\omega)$, where ω is the optical angular frequency and $\tilde{E}(\omega)$ the frequency component of the field. Figure 1(b) shows a sketch of the experiment which allowed us to measure $I_E(\omega)$ where the spectrometer is a scanning Fabry-Perot interferometer.

The relation between $S_{\delta\nu}(f)$ and $I_E(\omega)$ is written [16,22]

$$I_E(\omega) = E_0^2 \int_0^\infty \cos[(\omega_0 - \omega)\tau] \times \left\{ \exp \left[-4 \int_0^\infty S_{\delta\nu}(f) \frac{\sin^2(\pi f \tau)}{f^2} df \right] \right\} d\tau. \quad (3)$$

Again, some steps of the calculation are given in Appendix A.

The noise spectrum $S_{\delta\nu}(f)$ can generally be represented in a polynomial form in which the constant term h_0 (white noise) and the h_{-1}/f term are the main contributions.

When Eq. (3) is applied to the white noise case, $S_{\delta\nu}(f) = h_0$, and a Lorentzian function is obtained:

$$I_E(\omega) = \frac{E_0^2}{2} \frac{1}{i(\omega - \omega_0) + 2\pi^2 h_0} + \text{c.c.} \quad (4)$$

The relation between Γ , the HWHM of the line, and the white noise coefficient h_0 is thus

$$\Gamma = 2\pi^2 h_0. \quad (5)$$

Here Γ is expressed in rad/s. When Eq. (3) is applied to the flicker noise case, $S_{\delta\nu}(f) = h_{-1}/f$, one obtains

$$I_E(\omega) = E_0^2 \int_0^\infty \cos[(\omega_0 - \omega)\tau] \times \left\{ \exp \left[-4h_{-1} \int_0^\infty \frac{\sin^2(\pi f \tau)}{f^3} df \right] \right\} d\tau. \quad (6)$$

The problem here is that the integral $J = \int_0^\infty [\sin^2(\pi f \tau)/f^3] df$ is not convergent. The physical way to solve it is to notice that J is a function of time τ and that the minimum frequency which can be observed during this time is $1/\tau$. One thus obtains $J = (\pi\tau)^2 0.022561$ which gives the Gaussian function

$$I_E(\omega) = E_0^2 \frac{\sqrt{\pi}}{\sigma} e^{-(\omega_0 - \omega)^2 / \sigma^2}. \tag{7}$$

The variance σ^2 is linked to h_{-1} by the relation

$$\sigma^2 = 3.56h_{-1}. \tag{8}$$

When Eq. (3) is applied to the mixed case, $S_{\delta\nu}(f) = h_0 + h_{-1}/f$, one obtains

$$I_E(\omega) = \frac{E_0^2}{2} \int_0^\infty e^{i(\omega_0 - \omega)\tau - \Gamma\tau - (\sigma\tau/2)^2} d\tau + c.c. \tag{9}$$

This result can be manipulated to give

$$I_E(\omega) = E_0^2 \frac{\sqrt{\pi}}{\sigma} K(X, Y), \tag{10}$$

where $K(X, Y)$ is the Voigt function [23] defined by

$$K(X, Y) = \frac{Y}{\pi} \int_{-\infty}^\infty \frac{e^{-t^2} dt}{(X - t)^2 + Y^2}. \tag{11}$$

Here, $X = (\omega - \omega_0) / \sigma$, $Y = \Gamma / \sigma$, and $t = \sigma\tau/2 + iX + Y$, with the same relation between Γ and h_0 , σ , and h_{-1} as before. Equation (10) allows us to compute the spectrum from h_0 and h_{-1} which are obtained from noise measurements. One originality of this article rests on formula (10), its subsequent experimental verification, and its demonstration from first principles.

B. Experimental test

In order to check the validity of the Voigt formula to describe the line shape, we have measured the spectrum of a standard single-mode distributed feedback (DFB) semiconductor laser³ used in telecommunications at 1.55 μm . The experimental setup is schematically described in Fig. 1(b). The laser temperature is stabilized. The Fabry-Perot spectrometer has a sweep time of 9 ms and its feedback into the laser is kept as weak as possible ($<10^{-7}$). Its bandpass is 3.5 MHz and its free spectral range is 300 MHz. These characteristics add to the uncertainty of the measurements which essentially arises from the $1/f$ noise.

Figure 2 shows examples of a comparison between three measured line profiles and theoretical Voigt profiles.

The success in such fits for various values of the injection current (and also for different laser temperature T) led us to make several runs in order to draw curves like those represented in Fig. 3 which shows the variation of the fit parameters Γ and σ versus the laser power P for a fixed temperature. We have verified that σ slightly increases with temperature; however, the variation was too small to be really significant as compared to the uncertainty of our measurements. In our first verification of the validity of the description of laser lines by a Voigt function, the agreement between theory and experiment is satisfying: The experimen-

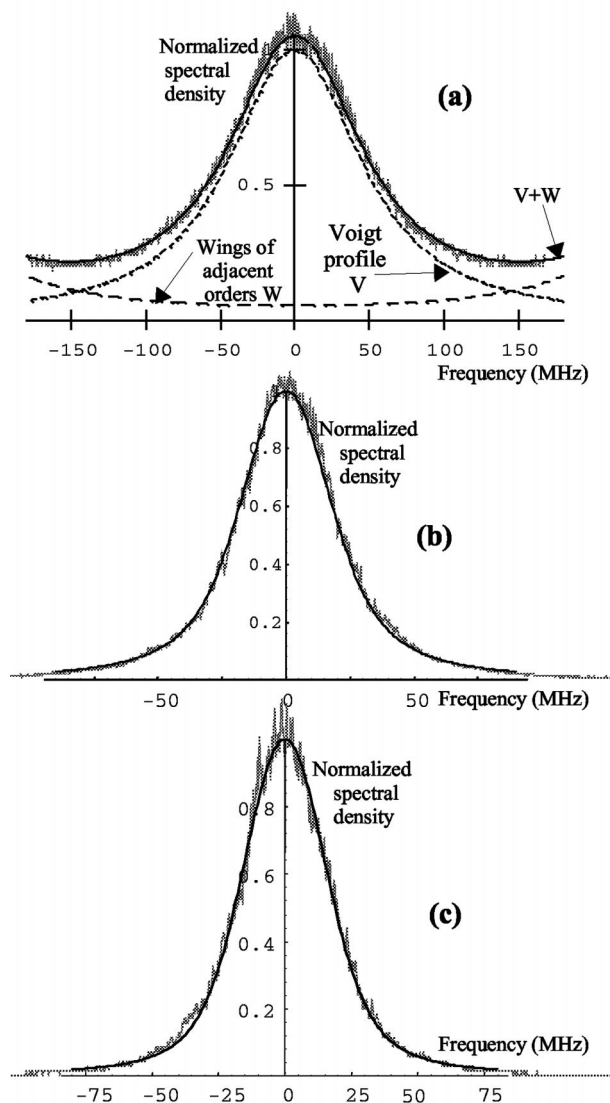


FIG. 2. Three examples of the line profile measured at $T \approx 31^\circ\text{C}$, using the mounting in Fig. 1(b). The experimental result is the noisy line in gray; the theoretical fit is the black solid line. In (a), the full width at half maximum is $\text{FWHM} = 108\text{ MHz}$, and the laser power is $P = 307\ \mu\text{W}$. The Fabry-Perot free spectral range being 300 MHz, the measured profile results from the sum of the Voigt function V and the wings W of the neighboring orders as indicated in the figure. In (b), $\text{FWHM} = 45\text{ MHz}$ and $P = 835\ \mu\text{W}$. In (c), $\text{FWHM} = 40\text{ MHz}$ and $P = 1.55\text{ mW}$.

tal points in Fig. 3 show that Γ varies like $1/P$ in agreement with already known theory. It shows also that σ displays a slower decrease with the intensity, also in agreement with previously known behavior [15].

III. DESCRIPTION OF THE LASER SPECTRUM

Starting from frequency noise measurements, we have computed the laser line and found that a Voigt function is compatible with the simultaneous white and flicker noises.

³The laser is a massive InP/InGaAsP buried double-heterostructure distributed feedback laser.

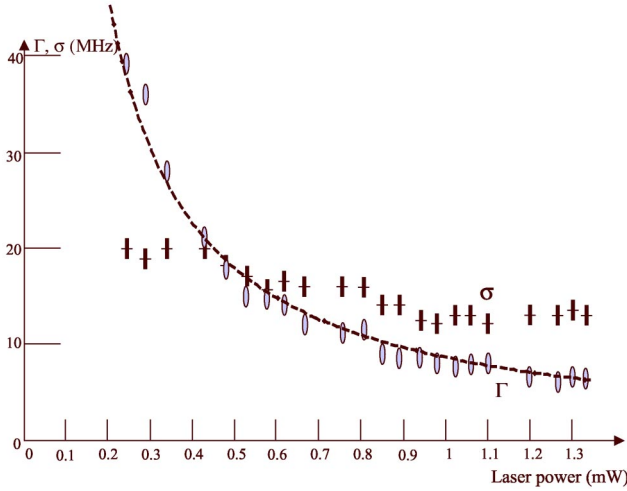


FIG. 3. Fit parameters Γ (ovals) and σ (crosses) in MHz vs the laser power P in mW. The variation of σ is not regular, while Γ follows the a/P curve, with $a \approx 8.7$ mW MHz. Here $T \approx 22$ °C. For $T \approx 31$ °C, we found $a \approx 11$ mW MHz.

We have then experimentally tested the formula and found a nice agreement with the line shapes and this Voigt profile. It remains now to find also that this Voigt function can be found from the electromagnetism of the laser. This is done below, where we show that the homogeneous part, the Lorentzian, is in fact the laser Airy function and the inhomogeneous part, the Gaussian, originates from the noise of the resonance frequency.

A. Laser Airy function

In the frequency domain, the laser field is the *response* of the device, the laser, to its sources. These sources are the spontaneous emission and the pumping process. It has already been demonstrated [20,21] that applying Maxwell equations and boundary conditions to a frequency component of the field gives the laser transfer function, or the laser Airy function:

$$\tilde{E} = \frac{\tilde{S}_e}{1 - e^{-L+g} e^{-i\phi}}. \quad (12)$$

\tilde{E} represents a component at frequency ω of the laser field and \tilde{S}_e the effective source at that frequency (amplified spontaneous emission). The loss term is written as e^{-L} . The active medium is represented by $\bar{\beta}$ including the dispersion and gain. ℓ being the laser length, the exponential term is split into its real and imaginary parts, $e^{-2i\bar{\beta}\ell} = e^{-2i\bar{\beta}'\ell} e^{2\bar{\beta}''\ell} = e^{-i\phi} e^g$ in order to explicitly show the gain g and the cumulated round trip phase ϕ :

$$\phi = 2\bar{\beta}''\ell = 2\omega n\ell/c, \quad (13)$$

where n is the refraction index. The saturated quantities such as $\bar{\beta}$ have been averaged with respect to the saturating intensity.

The optical Airy function is easily calculated for a Fabry-Perot interferometer or a Fabry-Perot laser. It can also be obtained for DFB lasers (see Appendix B) and has the same basic structure. In the following, we will thus use the simple formula (12).

In the single-mode case, the spectrum is centered around the resonance angular frequency ω_0 , which is given from $\phi = Q2\pi$ by

$$\omega_0 = Q2\pi \frac{c}{2n(\omega_0)\ell}. \quad (14)$$

The associated spectral density is

$$\tilde{I}(\omega) = \frac{|\tilde{S}_e|^2}{(1 - e^{-L+g})^2 + 4e^{-L+g} \sin^2(\phi/2)}. \quad (15)$$

If one considers the line shape of a single-mode laser around the central resonance frequency, ϕ remains very small and the approximation $4 \sin^2(\phi/2) \approx \phi^2$ can be used. In this case, expression (15) leads to the Lorentzian shape

$$\tilde{I} = \frac{c^2 |\tilde{S}_e|^2}{4\ell^2 n_g^2 e^{-L+g} \Gamma^2 + (\omega - \omega_0)^2}, \quad (16)$$

where the half width at half maximum Γ is

$$\Gamma = \frac{c}{2\ell n_g} \frac{1 - e^{-L+g}}{e^{-(L+g)/2}}, \quad (17)$$

and n_g is the group index around ω_0 . In the stationary regime, the saturating intensity \mathbf{I} can be easily computed for a Lorentzian line [19,20]:

$$\mathbf{I} = \int \tilde{I} d\omega / 2\pi = \frac{c^2 |\tilde{S}_e|^2}{4\ell^2 n_g^2 e^{-L+g} 2\Gamma}. \quad (18)$$

Note that \mathbf{I} does not depend on the frequency. We will conform to the usage and introduce the saturation intensity I_s in order to work with a normalized quantity $P = \mathbf{I}/I_s$. I_s is such that the gain $g = g_0/(1 + \mathbf{I}/I_s)$ is divided by 2 when $\mathbf{I} = I_s$.

When the laser is far from the threshold, P is very close to the power P_L which is obtained when the saturated gain $g = g_0/(1 + P)$ compensates exactly for losses ($P_L = g_0/L - 1$ can be termed Lamb's solution). In that case, the equality $g_0 = L$, where $P_L = 0$, defines the oscillation threshold of the laser. Anyway, even when the laser is close to the threshold, the gain g is very close to the losses L and the approximation $e^{-L+g} \approx 1$ holds everywhere but in the expression $1 - e^{-L+g} \approx L - g$.

Using Eq. (18), the approximated linewidth (17) is related to the saturating power P :

$$\Gamma \approx \frac{c}{2\ell n_g} (L - g) = \frac{c^2}{(2\ell n_g)^2 2I_s} \frac{|\tilde{S}_e|^2}{P}. \quad (19)$$

It is inversely proportional to P .

When the source term is expressed as

$$|\tilde{S}_e|^2 = K \frac{g_0}{1+P}, \quad (20)$$

where K is a constant, one can easily compute P . The result is

$$P = \frac{g_0 - L}{2L} + \frac{1}{2L} \sqrt{(g_0 - L)^2 + \frac{cK}{\ell n_g I_s} L g_0}. \quad (21)$$

This expression correctly describes the laser intensity. It can be tested around the threshold, especially for semiconductor lasers and for high-loss fiber lasers. Note that when the spontaneous emission is neglected ($K=0$), it gives back P_L .

B. Population fluctuations and the Voigt function

The homogeneous part of the line shape is described by the laser Airy function as shown above. This line is centered around the central frequency ω_0 . Now this function has been calculated for a single value of N , the population difference. It should be recalled that N is a random variable with different realizations in the frequency domain, each realization having a statistical weight or a probability $\mathcal{P}(N)$. It follows that the line shape results from a convolution of the Airy function and the probability function corresponding to each of these realizations of N . These fluctuations introduce a noise on every physical quantity in the laser (gain, linewidth, for instance) but the stronger effect occurs on the position of the resonance frequency ω_0 : For each value of N , the Airy function is centered around $\omega_0 = \omega_0(N)$ with the probability $\mathcal{P}(N)$. This probability is essentially Gaussian, which corresponds to the intrinsic electronic $1/f$ noise and also to the different causes of technical noises [6].

The spectral profile (16) is then averaged over the different probabilities of N :

$$\langle \tilde{y}(N) \rangle_N = \int_{-\infty}^{\infty} \frac{c^2 |\tilde{S}_e|^2}{4\ell^2 n_g^2 e^{-L+g}} \frac{\mathcal{P}(\delta N) d(\delta N)}{\Gamma^2 + [\omega - \omega_0(N)]^2}, \quad (22)$$

where $\delta N = N - \bar{N}$ and \bar{N} is the most probable value.

Let us note that the laser intensity corresponding to the averaged value $\langle \tilde{y}(N) \rangle_N$ remains the same as the intensity before in Eq. (18), simply because $\mathcal{P}(\delta N)$ is a normalized probability. The saturating intensity is thus only due to the homogeneous part of the laser line. In order to see how δN acts on $\omega_0(N)$, let us first write the gain g and the refraction index n of the medium under the compact form

$$g = AN, \quad n = n_1 + BN, \quad (23)$$

where A , B , and n_1 are constants.

Now we assume the simple expression for the saturated population (for a homogeneous medium)

$$N = \frac{N_{ns}}{1+P}. \quad (24)$$

Here N_{ns} stands for the nonsaturated value of N . Note that in the laser regime $P \simeq P_L$. It follows that the saturated gain and the saturated index are written

$$g = A \frac{N_{ns}}{1+P}, \quad n = n_1 + B \frac{N_{ns}}{1+P}. \quad (25)$$

The angular frequency at resonance (always for the single mode laser) is written, for a given value of N [see Eq. (14)],

$$\omega_0(N) = Q2\pi \frac{c}{2\ell n(N)}, \quad (26)$$

where Q is an integer. The value of $\omega_0(N)$ around the reference $\omega_0(\bar{N})$ is obtained from a Taylor expansion:

$$\omega_0(N) = \omega_0(\bar{N}) - Q2\pi \frac{c}{2\ell} \frac{dn}{n^2(\bar{N})} = \omega_0(\bar{N}) \left[1 - \frac{\delta n}{n(\bar{N})} \right]. \quad (27)$$

Let us note that a difference $\omega_0(N) - \omega_0(\bar{N})$ of the same order of magnitude as the laser linewidth is obtained for a very small variation of $\delta n/n(\bar{N})$ due to the large value of Q . For instance, if $\omega_0(\bar{N}) \simeq 10^{15}$ rad/s, a variation $\delta n/n(\bar{N}) \simeq 10^{-8}$ only leads to $[\omega_0(N) - \omega_0(\bar{N})]/2\pi = 10$ MHz. It is thus necessary to be very cautious in playing with approximations.

In order to obtain the variation δn of the index of refraction when N varies, one writes [see Eq. (19)]

$$n = n_1 + \frac{B}{A} g = n_1 + \frac{B}{A} \left[L - \frac{c|\tilde{S}_e|^2}{2\ell n_g 2I_s P} \right]. \quad (28)$$

It follows that the index variation δn is related to the variation $\delta N = N - \bar{N}$ of N around \bar{N} by

$$\delta n = - \frac{B}{A} \frac{d}{dN} \left[\frac{c|\tilde{S}_e|^2}{2\ell n_g 2I_s P} \right] \delta N. \quad (29)$$

We are now in position to introduce Henry's factor [13,25,26]

$$\alpha_H = \frac{B}{A} \quad (30)$$

and another factor, which is also characteristic of the amplifying medium,

$$\alpha' = \frac{d}{dN} \left[\frac{c|\tilde{S}_e|^2}{2\ell n_g 2I_s P} \right], \quad (31)$$

in order to write the formula

$$\delta n = - \alpha_H \alpha' \delta N. \quad (32)$$

Let us note that a neglect of the spontaneous emission $|\tilde{S}_e|^2$ leads to $\alpha' = 0$, or a zero variation of the refraction index. This is because P becomes P_L which clamps the saturated population $N/(1+P_L)$ from the relation $g=L$ in this case. One thus obtains

$$\omega_0(N) - \omega_0(\bar{N}) = \omega_0(\bar{N}) \frac{\alpha_H \alpha'}{n(N_0)} \delta N. \quad (33)$$

We recover in formulas (32) and (33) the usual frequency shift from the transparency to the threshold. The index dif-

ference in Eq. (32) has been measured in [27] with a precision of 1%. Expression (33) is introduced in the equation for the mean profile (22) where we make the approximation $e^{-L+g} \simeq 1$:

$$\begin{aligned} \langle \tilde{y}(N) \rangle_N &= \frac{c^2 |\tilde{S}_e|^2}{4\ell^2 n_g^2} \int_{-\infty}^{\infty} \frac{\mathcal{P}(\delta N) d(\delta N)}{\Gamma^2 + [\omega - \omega_0(\bar{N}) - \omega_0(\bar{N})\alpha_H \alpha' / n(\bar{N}) \delta N]^2}. \end{aligned} \quad (34)$$

Let us write now that δN follows a Gaussian probability law

$$\mathcal{P}(N) = \frac{e^{-(\delta N/\sigma_1)^2/2}}{\sigma_1 \sqrt{2\pi}}. \quad (35)$$

$\mathcal{P}(N)$ is characterized by its variance (or its second moment) σ_1^2 . One sees now that $\langle \tilde{y}(N) \rangle_N$ is the convolution of a Lorentzian with a Gaussian—i.e., a Voigt profile.

In order to conform to the notation associated to the Voigt function, let us introduce

$$t = \frac{\delta N}{\sigma_1 \sqrt{2}} \quad (36)$$

and

$$d(\delta N) = \sigma_1 \sqrt{2} dt. \quad (37)$$

If we use the abbreviation

$$a = \frac{\omega_0(\bar{N})\alpha_H \alpha'}{n(\bar{N})} \quad (38)$$

and the normalized variables:

$$Y \equiv \frac{\Gamma}{a\sigma_1 \sqrt{2}}, \quad X \equiv \frac{\omega - \omega_0(\bar{N})}{a\sigma_1 \sqrt{2}}, \quad (39)$$

the expression for the averaged spectral profile becomes

$$\langle \tilde{y}(N) \rangle_N = \frac{c^2 |\tilde{S}_e|^2}{4\ell^2 n_g^2} \frac{1}{2a^2 \sigma_1^2 \sqrt{\pi}} \int_{-\infty}^{\infty} \frac{e^{-t^2} dt}{Y^2 + [X - t]^2}. \quad (40)$$

In this formula, Y is the ratio of Lorentz to Gaussian widths. $\langle \tilde{y} \rangle$ is proportional to the Voigt function $K(X, Y)$ expressed in its standard form (11):

$$\langle \tilde{y}(N) \rangle_N = \frac{c^2 |\tilde{S}_e|^2}{4\ell^2 n_g^2} \frac{\sqrt{\pi}}{\sqrt{2} a \sigma_1 \Gamma} K(X, Y). \quad (41)$$

A comparison between Eqs. (10) and (41) and their associated symbols allows us to make the connection between the variance associated with population fluctuations and with the noise coefficient h_{-1} . However, it should be recalled that formula (41) contains more physics than formula (10) which expresses only the fact that the Voigt formula is compatible with the simultaneous white and $1/f$ noises.

The Voigt function usually characterizes spectral lines having an atomic origin; it follows that one can apply the same terminology to the laser line: (i) The “homogeneous”

part of the laser line is represented by its Airy function which is a Lorentzian around a resonance. This part corresponds to a single realization of the pump. (ii) The “inhomogeneous” part of the laser line is the Gauss function which describes the random character of the pump.

We have thus attained our goal in demonstrating formula (41). The difficulty here in dealing with the Gaussian part is that the origins of its variance span from the fundamental properties of the pumping process to the “technical noise.” It is well known that the linewidth is enlarged by a factor $(1 + \alpha_H^2)$ in the usual approximation of a Lorentzian line. In Eq. (41), we recover this broadening through the probabilistic nature of the resonant optical frequency. However, in Eq. (41), the factor is not as simple as before and could lead to another estimation of the α_H parameter. It is important to note that the uncertainty in measurements of α_H is usually bigger than 10% [15] which proves the limitations of the usual theory.

IV. CONCLUSION

In this paper we have first verified that a Voigt spectral profile is compatible with standard measurements of frequency noise in a single-mode laser: The Lorentzian part corresponds to the white noise part and the Gaussian part of the Voigt function corresponds to the $1/f$ noise part. The white noise arises from spontaneous emission and the flicker noise arises from fluctuations of the charge carriers or the pumping and from the “technical” noise. The formula does not include the intensity noise. We believe that the Voigt profile is characteristic of any single-mode laser. It follows that the spectrum of a metrological laser can be obtained from the measurement of the frequency noise coefficients.

We have then experimentally verified that the Voigt profile gives a very good fit to single-mode semiconductor lines and that the fit parameter Γ obeys an inverse power law while the second parameter σ varies more slowly with the power.

In the last section, we have put together the Airy function of the laser which becomes the homogeneous part of the Voigt function and the Gaussian probability distribution of the resonance frequency, which is its inhomogeneous part. In this work, only stationary lasers have been considered; the calculations are thus shorter, clearer, and more precise when they are done directly in the frequency domain. We have thus completed a synthesis of different phenomena all related to the spectral characteristics of the laser field.

It is clear from these results that a decrease of the laser spectral linewidth can be obtained only by a simultaneous and independent decrease of the noise coefficients h_0 and h_{-1} . h_0 can be decreased using high-quality resonators while h_{-1} can be decreased through mechanical, thermal, and acoustical stability, together with a pump process as stable as possible. In this respect, the electrical stability is fundamental. Our results confirm that the nature of the laser frequency noise depends upon the considered frequency band: (i) Essentially $1/f$ or white in frequency measurements and (ii) Gaussian near the center of the laser line spectrum, Lorentzian in the aisles. They also confirm that in some interfero-

metric experiments performed with the laser light, the result depends upon the measurement time, in agreement with Mercier [17].

APPENDIX A

The aim of this appendix is to describe the main steps which lead to Eqs. (2) and (3).

1. Relation between $S_{\delta\nu}(t)$ and $S_{\delta\nu}(f)$

The laser field is written in the scalar form

$$E(t) = E_0[1 + \varepsilon(t)]e^{i[\omega_0 t + \phi(t)]}. \quad (\text{A1})$$

$\varepsilon(t)$ is the amplitude noise which will be neglected in the following. $\phi(t)$ is the phase noise which makes the instantaneous frequency wander around the nominal frequency $\nu_0 = \omega_0/(2\pi)$. This field is injected into the interferometer and split into two parts inside the two arms. Both arms contain an optical fiber of known length. One arm contains a dephaser for fine-tuning and a polarization controller. L_1 and L_2 are the optical lengths of arms 1 and 2. The path difference $L_1 - L_2$ results in a time shift τ_d between the recombined fields E_1 and E_2 at the interferometer output: $\tau_d = (L_1 - L_2)/c$. The polarization controller is used to set the same polarization for E_1 and E_2 . The detector gives a signal which is proportional to the intensity of the interfering fields E_1 and E_2 :

$$\begin{aligned} i(t) &= \frac{K_D}{2} |\vec{E}_1 + \vec{E}_2|^2 \\ &= i_1 + i_2 + 2\sqrt{i_1 i_2} \cos[\omega_0 \tau_d + \phi(t + \tau_d) - \phi(t)]. \end{aligned} \quad (\text{A2})$$

The current $i(t)$ is then processed by an electronic spectrum analyzer which delivers $\tilde{S}_i(f)$, the Fourier transform of the autocorrelation function $R_i(\tau)$ of $i(t)$:

$$\tilde{S}_i(f) = T_{\text{Fourier}}\{R_i(\tau)\}, \quad (\text{A3})$$

with

$$R_i(\tau) = \langle i(t)i(t + \tau) \rangle. \quad (\text{A4})$$

Note that $\tilde{S}_i(f)$ is also the modulus square of the Fourier transform of $i(t)$.

We are first looking at the relation between the power spectral density of frequency noise $S_{\delta\nu}(f)$ and the power spectral density of the input current $\tilde{S}_i(f)$ given by the spectrum analyzer.

The autocorrelation function $R_i(\tau)$ of the photocurrent $i(t) = i_1(t) + i_2(t)$ is obtained by computing the mean value over the time t of the following expression:

$$\begin{aligned} R_i(\tau) &= (i_1 + i_2)^2 + (i_1 + i_2) \sqrt{i_1 i_2} \langle e^{i[\omega_0 \tau_d + v]} + e^{-i[\omega_0 \tau_d + v]} \\ &\quad + e^{i[\omega_0 \tau_d + w]} + e^{-i[\omega_0 \tau_d + w]} \rangle + i_1 i_2 \langle \{ e^{i[\omega_0 \tau_d + v]} + e^{-i[\omega_0 \tau_d + v]} \} \\ &\quad \times \{ e^{i[\omega_0 \tau_d + w]} + e^{-i[\omega_0 \tau_d + w]} \} \rangle, \end{aligned} \quad (\text{A5})$$

with the notation

$$v = \phi(t + \tau_d) - \phi(t), \quad (\text{A6})$$

$$w = \phi(t + \tau + \tau_d) - \phi(t + \tau). \quad (\text{A7})$$

The reference angle $\omega_0 \tau_d$ is adjusted in such a way that

$$\cos[\omega_0 \tau_d + \phi(t + \tau_d) - \phi(t)] = \sin[\phi(t + \tau_d) - \phi(t)]. \quad (\text{A8})$$

In this case, the interferometer is used as a phase-amplitude converter. We work also within the hypothesis of weak deviations v and w . The experimental condition is $\tau_d \ll 1/\Gamma$.

The frequency deviation is linked to the phase variation during the time t by the relation

$$\delta\phi(t, \tau) = 2\pi \int_t^{t+\tau} \delta\nu(t') dt'. \quad (\text{A9})$$

The correlation function of the frequency fluctuation $\delta\nu(t)$ is defined for a stationary process

$$R_{\delta\nu}(t', t'') = \langle \delta\nu(t') \delta\nu(t'') \rangle = R_{\delta\nu}(t' - t''). \quad (\text{A10})$$

Note that the dimension of $R_{\delta\nu}(t' - t'')$ is Hz^2 or T^{-2} .

In the course of the calculation of $R_i(\tau)$, the following general identity is used:

$$\begin{aligned} &\int_a^b \int_c^d R_{\delta\nu}(t' - t'') dt' dt'' \\ &= \int_0^{(a-b)} R_{\delta\nu}(-X - a + c) dX [(b - a + d - c)/2 - X] \\ &\quad + \int_0^{(d-c)} R_{\delta\nu}(X - a + c) dX [(b - a + d - c)/2 - X]. \end{aligned} \quad (\text{A11})$$

We use also the familiar mean value for a Gaussian process:

$$\langle e^{i\phi(t)} \rangle = e^{-4\pi^2 \langle \phi(t) \rangle^2 / 2}. \quad (\text{A12})$$

After some calculations, one finds

$$\begin{aligned} R_i(\tau) &= (i_1 + i_2)^2 - 2i_1 i_2 \left[-8\pi^2 \int_0^{\tau_d} [R_{\delta\nu}(X + \tau) \right. \\ &\quad \left. + R_{\delta\nu}(-X + \tau)] [\tau_d - X] dX \right]. \end{aligned} \quad (\text{A13})$$

The spectrum analyzer gives, as a result, $\tilde{S}_i(f)$, the Fourier transform of $R_i(\tau)$:

$$\tilde{S}_i(f) = \int_{-\infty}^{\infty} R_i(\tau) e^{-2i\pi f \tau} d\tau. \quad (\text{A14})$$

We will use the relation of the definition of the power spectral density of frequency noise (T_{Fourier} of the frequency fluctuation correlation):

$$S_{\delta\nu}(f) = \int_{-\infty}^{\infty} e^{-2i\pi f\tau} R_{\delta\nu}(\tau) d\tau. \quad (\text{A15})$$

Note that the dimension of $S_{\delta\nu}(f)$ is in Hz or T^{-1} [$S_{\delta\nu}(f)$ is commonly expressed in Hz^2/Hz]. We obtain the desired result

$$\tilde{S}_i(f) = (i_1 + i_2)^2 \delta(f) + 16i_1 i_2 S_{\delta\nu}(f) \frac{\sin^2(\pi f \tau_d)}{f^2}.$$

For $f \neq 0$,

$$S_{\delta\nu}(f) = \frac{1}{16i_1 i_2 \sin^2(\pi f \tau_d)} \tilde{S}_i(f). \quad (\text{A16})$$

This result links the measured quantity $\tilde{S}_i(f)$ to the quantity $S_{\delta\nu}(f)$ which characterizes the frequency fluctuation of the field. It is clear that when the angle $\pi f \tau_d$ is small, the approximation $\sin^2(\pi f \tau_d) \simeq (\pi f \tau_d)^2$ can be used. In this case f^2 disappears and $S_{\delta\nu}(f)$ is directly represented by $\tilde{S}_i(f)$.

2. Relation between $S_{\delta\nu}(f)$ and the optical spectrum $I_E(\omega)$

We have used the relation between $S_{\delta\nu}(f)$ and the optical spectrum $I_E(\omega) = \tilde{E}(\omega) \tilde{E}^*(\omega)$, where ω is the optical frequency and $\tilde{E}(\omega)$ the frequency component of the field.

Let us give now the main steps which lead to this relation. The quantities which are used are the same as before.

The strategy is the following.

(i) $I_E(\omega)$ is linked to the temporal correlation $R_E(\tau)$ through the Fourier transform (Wiener-Khinchin theorem):

$$\begin{aligned} I_E(\omega) &= \text{Re} \left\{ \int_{-\infty}^{\infty} R_E(\tau) e^{-i\omega\tau} d\tau \right\} \\ &= \text{Re} \left\{ \int_{-\infty}^{\infty} \langle E^*(t) E(t+\tau) \rangle e^{-i\omega\tau} d\tau \right\}. \end{aligned} \quad (\text{A17})$$

(ii) Now, for a Gaussian process, $R_E(\tau)$ can be written as

$$R_E(\tau) = \langle E^*(t) E(t+\tau) \rangle = e^{i\omega_0\tau} e^{-\sigma^2/2\bar{I}}, \quad (\text{A18})$$

where

$$\sigma^2 = \sigma^2(\tau) = \langle [\phi(t+\tau) - \phi(t)]^2 \rangle, \quad (\text{A19})$$

and \bar{I} is the intensity. One obtains

$$I_E(\omega) = \bar{I} \int_{-\infty}^{\infty} e^{-\sigma^2/2} \cos[(\omega_0 - \omega)\tau] d\tau. \quad (\text{A20})$$

(iii) The following step is to relate σ^2 to $R_{\delta\nu}(\tau)$, the temporal correlation of $\delta\nu(t)$. One obtains

$$\sigma^2 = 2 \int_0^{\tau} (\tau-t) R_{\delta\nu}(t) dt. \quad (\text{A21})$$

(iv) Finally, one remembers that the power spectral density of frequency noise $S_{\delta\nu}(f)$ and the temporal correlation $R_{\delta\nu}(\tau)$ are Fourier transforms of each other.

When the calculation is performed following these steps, one finds the desired relation (3).

APPENDIX B

The aim of this appendix is to briefly describe the Airy function of the DFB laser.

The method is to start from the coupled wave theory [24] where a frequency component of the laser field is written with the standard notation:

$$\begin{aligned} \tilde{E}(z) &= [A_1 e^{-iqz} + rB_2 e^{iqz}] e^{-i\beta_0 z} + s_1(z) \\ &\quad + [rA_1 e^{-iqz} + B_2 e^{iqz}] e^{i\beta_0 z} + s_2(z). \end{aligned} \quad (\text{B1})$$

Here A_1 , rB_2 , rA_1 , and B_2 are the progressive longitudinal slowly varying envelopes of the field, r the reflectance of the Bragg grating,

$$r = 2\beta \frac{q - \Delta\beta}{\kappa} = -\frac{\kappa}{2\beta q + \Delta\beta}, \quad (\text{B2})$$

with $\Delta\beta = \beta' - m\pi/\Lambda$, β' being the real part of the propagation constant of the medium, Λ the grating period, and m an integer which minimizes $\Delta\beta$. One has also $\beta_0 = m\pi/\Lambda$ and

$$q = \left[\Delta\beta^2 - \frac{\kappa^2}{4\beta^2} \right]^{1/2}, \quad (\text{B3})$$

κ being a coefficient which describes the coupling between the transverse and longitudinal parts of the field.

The symbols $s_1(z)$ and $s_2(z)$ represent the local spontaneous emission (source terms). When boundary conditions are applied, one finds

$$\begin{aligned} A_1 &= \frac{S_1}{1 - r_1^2 e^{-2i(q-\beta_0)\ell}}, \\ B_2 &= \frac{S_2}{1 - r_1^2 e^{-2i(q-\beta_0)\ell}}, \end{aligned} \quad (\text{B4})$$

where r_1 is the complex effective reflectance:

$$r_1 = \frac{(\beta_{ext} - \beta_0 - q) + r(\beta_{ext} + \beta_0 - q) e^{i\beta_0 \ell}}{\beta_{ext} + \beta_0 + q + r(\beta_{ext} - \beta_0 + q) e^{-i\beta_0 \ell}}. \quad (\text{B5})$$

Here β_{ext} is the propagation constant of the external medium (if this medium is air, $\beta_{ext} = \omega/c$). The source terms S_1 and S_2 in Eqs. (B4) depend in a complicated way on the laser structure: Their expressions are not important here. The main conclusion is that expressions (B4) have the same structure as Eq. (12).

- [1] Y. Yamamoto, S. Saito, and T. Mukai, *IEEE J. Quantum Electron.* **QE-19**, 47 (1983).
- [2] K. Kikuchi, *IEEE J. Quantum Electron.* **QE-25**, 684 (1989).
- [3] P. Tremblay, C. S. Turcotte, M. Bondiou, J. Genest, M. Allard, P. Lévesque, J. P. Bouchard, C. Latrasse, M. Poulin, and M. Têtu, in *Proceedings of the 6th Symposium on Frequency Standards and Metrology*, 9–14 September 2001, Fife, Scotland, UK, edited by P. Gill (World Scientific, Singapore, 2002).
- [4] J. J. Brophy, *J. Appl. Phys.* **38**, 2465 (1967).
- [5] G. Tenchio, *Electron. Lett.* **12**, 562 (1976).
- [6] R. J. Fronen, Ph.D. thesis, Eindhoven University, 1990.
- [7] W. H. Burkett, B. Lü, and M. Xiao, *IEEE J. Quantum Electron.* **QE-33**, 2111 (1997).
- [8] G. P. Agrawal and R. Roy, *Phys. Rev. A* **37**, 2495 (1988).
- [9] Ph. Laurent, A. Clairon, and Ch. Bréant, *IEEE J. Quantum Electron.* **QE-25**, 1137 (1989).
- [10] A. Dandridge and H. F. Taylor, *IEEE J. Quantum Electron.* **QE-18**, 1738 (1982).
- [11] D. Welford and A. Mooradian, *Appl. Phys. Lett.* **40**, 560 (1982).
- [12] K. Vahala and A. Yariv, *Appl. Phys. Lett.* **43**, 140 (1983).
- [13] C. H. Henry, *IEEE J. Quantum Electron.* **QE-18**, 259 (1982).
- [14] M. Sargent, M. O. Scully, and W. Lamb, Jr., *Laser Physics* (Addison-Wesley, Reading, MA, 1974).
- [15] M. Osinski and J. Buus, *IEEE J. Quantum Electron.* **QE-23**, 9 (1987).
- [16] B. Fermigier and M. Têtu, *Proc. SPIE* **3415**, 164(1998).
- [17] L. D. Mercer, *J. Lightwave Technol.* **9**, 485 (1991).
- [18] M. J. O'Mahony and I. D. Henning, *Electron. Lett.* **19**, 1000 (1983).
- [19] G. M. Stéphan, *Phys. Rev. A* **55**, 1371 (1997).
- [20] G. M. Stéphan, *Phys. Rev. A* **58**, 2467 (1998).
- [21] M. Bondiou, R. Gabet, G. M. Stéphan, and P. Besnard, *J. Opt. Soc. Am. B* **2**, 41 (2000).
- [22] D. S. Elliot, R. Roy, and S. J. Smith, *Phys. Rev. A* **26**, 12 (1982).
- [23] The Voigt function is the real part of the complex probability function. See V. N. Faddeyeva and N. M. Terent'ev, *Tables of the Function $w(z)=e^{-z^2}[1+2i/\sqrt{\pi}\int_0^z e^{-t^2} dt]$ for Complex Argument* (Pergamont Press, Oxford, 1961). It is linked to the plasma dispersion function. See B. D. Fried and S. D. Conte, *The Plasma Dispersion Function, the Hilbert Transform of the Gaussian* (Academic Press, New York, 1961). See also B. H. Armstrong, *J. Quant. Spectrosc. Radiat. Transf.* **7**, 61 (1967).
- [24] G. P. Agrawal and N. K. Dutta, *Semiconductor Lasers*, 2nd ed. (Van Nostrand Reinhold, New York, 1993), Chap. 7. Seminal papers are H. Kogelnik and C. V. Shank, *Appl. Phys. Lett.* **18**, 152 (1971); *J. Appl. Phys.* **43**, 2327 (1972).
- [25] C. H. Henry, *J. Lightwave Technol.* **LT-4**, 298 (1986).
- [26] K. Vahala, L. C. Chiu, S. Margalit, and A. Yariv, *Appl. Phys. Lett.* **42**, 631 (1983).
- [27] C. H. Henry, R. A. Logan, and K. A. Bartness, *J. Appl. Phys.* **52**, 4457 (1981).